JOURNAL

of

STEEL CASTINGS RESEARCH

CONTENTS

A Microscopic Study of Rammed Sand Surfaces 1

SFSA Research Report No. 45—Packing of Steel Foundry Sands 8

Magnetic Properties of Cast Carbon Steels—Part II 9

The Effects of Residual Elements on the Magnetic Properties of Carbon Steel Castings 12

Abstracts of Fundamental Papers on Steel Casting Research 15

STEEL FOUNDERS' SOCIETY OF AMERICA

NUMBER 21 APRIL, 1961

JOURNAL OF STEEL CASTINGS RESEARCH

Number 21 April, 1961

TECHNICAL RESEARCH COMMITTEE, SFSA

V. E. ZANG, Unitcast Corporation, Chairman

F. H. ALLISON, JR., Foundry & Mill Machinery Division, Blaw Knox Company

H. H. BLOSJO, Malleable Iron Fittings Company

W. K. BOCK, National Malleable & Steel Castings Company

A. P. GUIDI, Texas Foundries, Inc.

G. F. HAISLUP, Electric Steel Castings Company

J. M. HATHAWAY, The Massillon Steel Casting Company

CHARLES LOCKE, Crucible Steel Casting Company

PHILIP McCAFFERY, General Metals Corporation

C. E. STULL, The Pelton Steel Casting Company

W. D. WALTHER, The Dayton Steel Foundry Company

DIRECTOR OF RESEARCH AND JOURNAL EDITOR
CHARLES W. BRIGGS

EDITORIAL STAFF

R. A. WILLEY,
Assistant Technical
and Research Director

CHARLES A. ROWE,
Assistant to the Technical
and Research Director

© by Steel Founders' Society of America, 1961

606 Terminal Tower Cleveland 13, Ohio

THE CIRCULATION OF THE JOURNAL IS RESTRICTED TO MEMBERS OF THE SOCIETY AND OTHERS AS AUTHORIZED BY THE BOARD OF DIRECTORS

A MICROSCOPIC STUDY OF RAMMED SAND SURFACES

by

J. B. Caine,* E. H. King, and J. S. Schumacher*****

Study of foundry sands in the past has been concentrated almost exclusively to the properties and behaviors of these sands as compacted masses. The smallest compacted mass normally used is the AFS 1¼-inch diameter specimen employed for high temperature testing. The usual compacted mass is 2 inches in diameter and 2 inches high, or over 6 cubic inches. The properties of such masses are important, but not to the exclusion of the small discontinuities that are known to exist in the relatively large compacted masses.

One important area of possible discontinuities is the surface of the compacted sand, specifically those surfaces of the gate system and the mold cavity. Surfaces differ from the mass as a whole from the atom on up and there is no reason to believe that the surfaces of a sand mass do not follow the general rule. One specific matter of concern has to do with rammed surface density, as density influences grain contact and contact influences bonding of individual surface grains. Small, but visible nonmetallic macroinclusions in the casting surface are a chronic problem of the industry. Small amounts of eroded sand are one possible source of these macroinclusions.

The problem is best illustrated by the three adjacent photomicrographs of Figure 1 which are composed of a cross section through the bottom, corner and side of a standard 2-inch diameter AFS test specimen after compaction by three rams of the 14-pound weight. The sand is a typical western bentonite-cereal bonded steel molding sand. The sand specimen has been invested with a thermo-setting plastic and polished as detailed in previous papers[1], [2]. The oblique illumination outlines the sand grains as white against the black plastic that has filled what were voids in the sand mass as rammed. The very loosely compacted sand grains at the surface in this low density sand are self-evident and are especially pronounced at the corner, even though the specimen was compacted to a relatively high level of 54 percent solid.

The magnification of Figure 1, 10 times, is a little too low for a detailed study of the relative densities of the surface and mass as a whole. However, at a higher magnification of 25 times it is possible by the grid method, details of which are given in the Appendix, to determine the density of any area of a sand mass. The photomicrographs of Figures 2 through 5 illustrate the relative densities of a number of rammed sand surfaces. Figure 3 indicates that

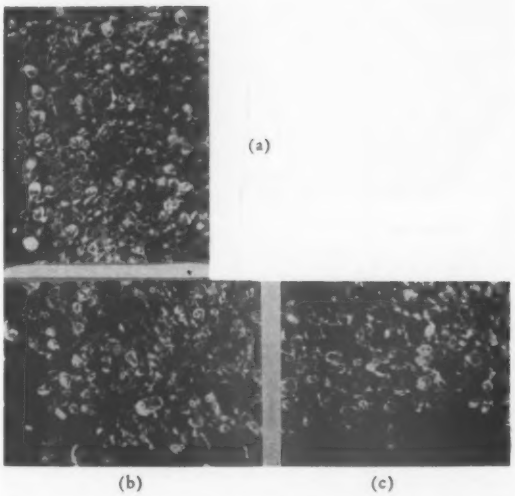

Figure 1—Surface of standard three-ram AFS specimen at bottom corner. Density by weight 54 percent solid. Steel molding sand, 6.7 psi green compression strength. 10X. (a) Average density 57 percent solid; density first .017 inch from surface, 45 percent solid. (b) Average density 55 percent solid; density first .017 inch from surface, 24 percent solid. (c) Average density 54 percent solid; density first .017 inch from surface, 41 percent solid.

a wash can seal the surface and prevent penetration at low metal static pressures. The possible susceptibility of the small unsupported "bridges" to spalling and erosion is also evident.

Figures 4 and 5 are particularly worrisome. They indicate that the density of the surface increases at a much slower rate than the mass as a whole with increasing energy of compaction. It may be quite difficult to compact the surface above a relatively low level.

The microdensities of Figures 1 through 5 can be roughly translated into more familiar properties of the mass as a whole. Figure 6 shows the relation between density and green hardness of two typical steel foundry sands compacted by jolting. Figures 7 and 8 show the relation between green hardness, green compressive strength and green permeability of rammed 2-inch AFS test specimens made of many different sands. Even though the relation of Figure 6 cannot be applied generally (it may vary with each sand and method of compaction) the very low densities of Figures 1 through 5 must correspond to very low green strength, very high permeability, in the order of 40 green hardness, 1 psi green strength, 600 permeability.

* Consultant, Cincinnati, Ohio; **President and ***Vice President, Hill and Griffith Company, Cincinnati, Ohio.

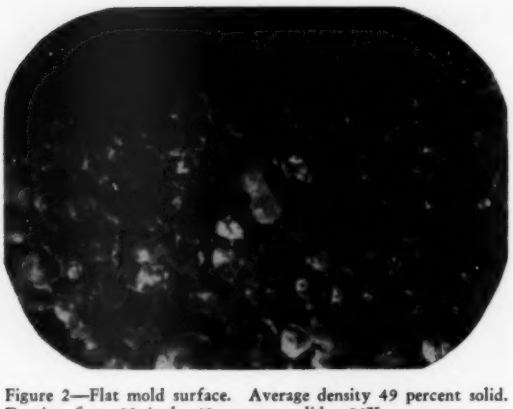

Figure 2—Flat mold surface. Average density 49 percent solid. Density first .02 inch, 40 percent solid. 25X.

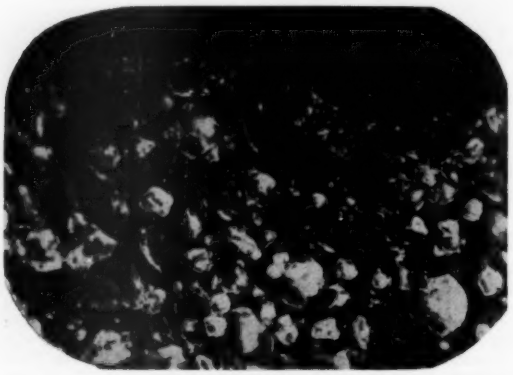

Figure 3—Same as Figure 2, but sprayed with 50 Baume silica wash. Note how wash bridges voids at surface. 25X.

Under such conditions, evidence indicates the possibility of molten metal erosion of individual sand grains, or small clusters of grains because of the low density of the compacted sand surfaces. Evidence also indicates that the mechanics of this erosion may be different from that usually considered by the industry as causing displaced sand by scabbing, buckling, or spalling.

Metal Erosion

Mercury was poured through small sand sprues in an effort to further study pure erosion by liquid metal without thermal influences. Successive pours of mercury were made through ¼-inch diameter sprues, 4 inches long. The eroded sand grains were separated from the mercury and weighed after each successive pour through the same sprue. The results are shown in the graphs of Figures 9 through 12. The amount of eroded sand is reported in milligrams. An idea as to the amount by volume is indicated by the black circles in Figure 13 that represent the size of 10, 50 and 100 milligram cones of sand when poured on a flat surface.

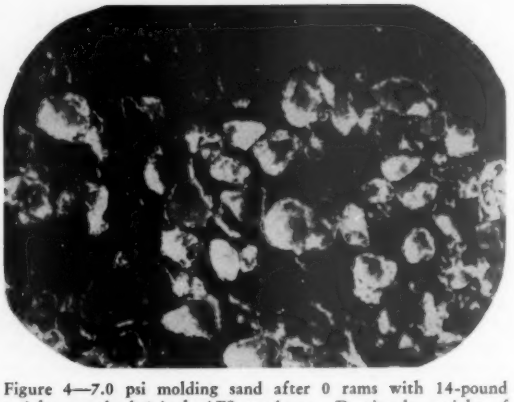

Figure 4—7.0 psi molding sand after 0 rams with 14-pound weight, standard 2-inch AFS specimen. Density by weight of 2-inch specimen 51 percent solid. Average microdensity 50 percent solid. Density first .02 inch, 38 percent solid. 25X.

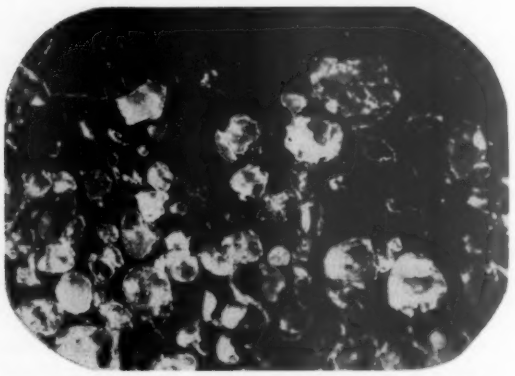

Figure 5—Same as Figure 4, but after 10 rams. Density by weight 57 percent solid. Average microdensity 55 percent solid. Density first .02 inch, 37 percent solid. 25X.

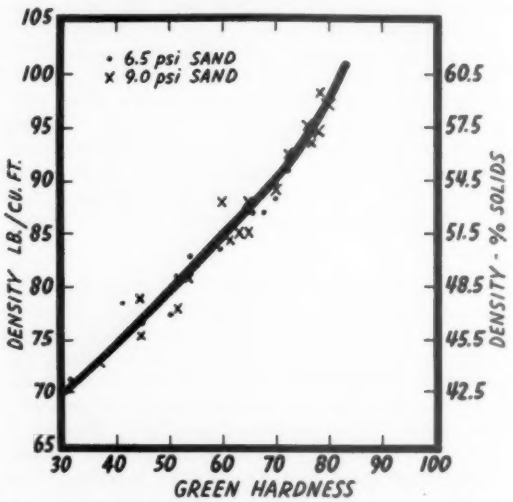

Figure 6—The relation between density and green hardness for two typical steel foundry sands compacted by jolting.

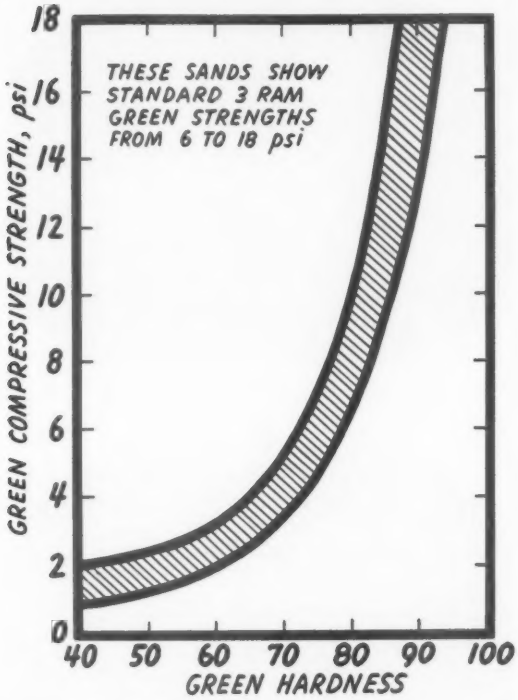

Figure 7—The relation between green compression strength and green hardness of 2-inch AFS test specimens made of many different sands.

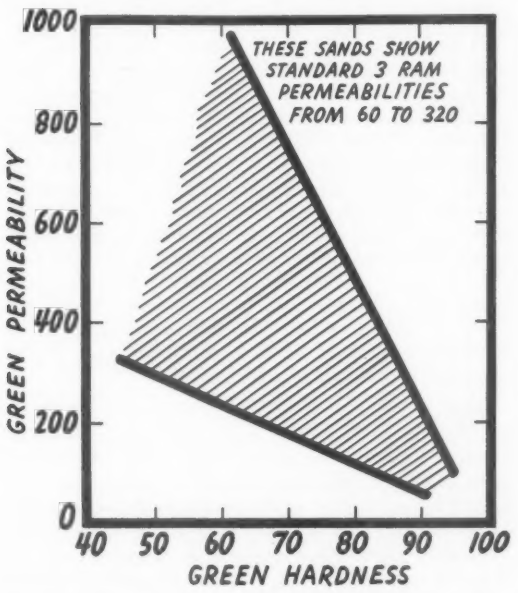

Figure 8—The relation between green permeability and green hardness of 2-inch AFS test specimens made of many different sands.

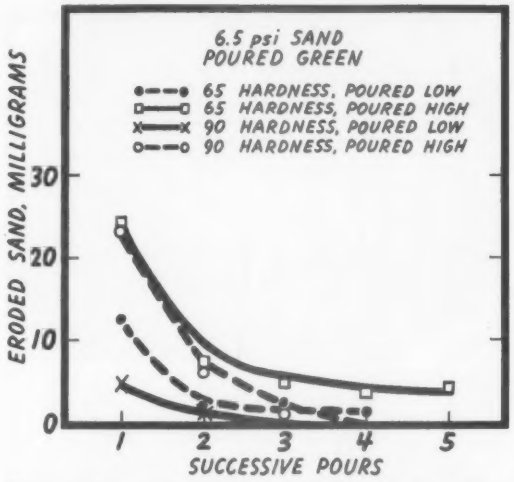

Figure 9—Amount of sand eroded with successive pours of 2.8 pounds of mercury through a ¼-inch diameter sprue.

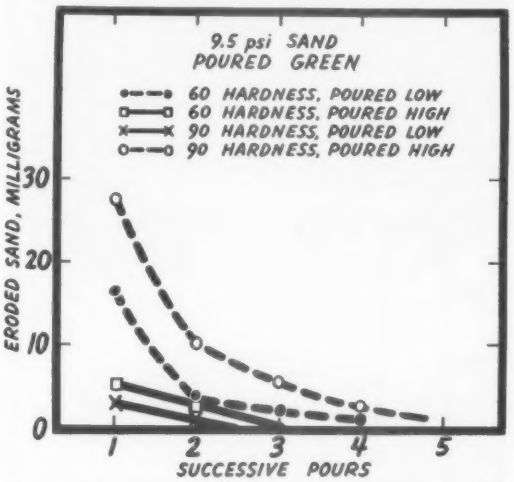

Figure 10—Amount of sand eroded with successive pours of 2.8 pounds of mercury through a ¼-inch diameter sprue.

The curves of Figures 9, 10, and 11 show maximum erosion with the first pour and a decrease in erosion with successive pours. The influence of bentonite content, ramming, height of ladle (beaker in the tests) above the sprue and air drying of the surface on pure erosion at room temperature are also shown in the graphs of Figures 9 - 12. The air dried curves of Figure 11 are probably the most significant, as a mold surface is dry immediately after contact with molten metal, if it did not dry out before contact. Figure 12 summarizes the data of Figures 9, 10 and 11 and shows the amount of erosion resulting from pouring 11 pounds of mercury through a ¼-inch diameter sprue in relation to green hardness of the sand mass. An appreciable amount of sand erodes even at 80 - 90 green hardness. At lower green hardness, erosion increases hyperbolically.

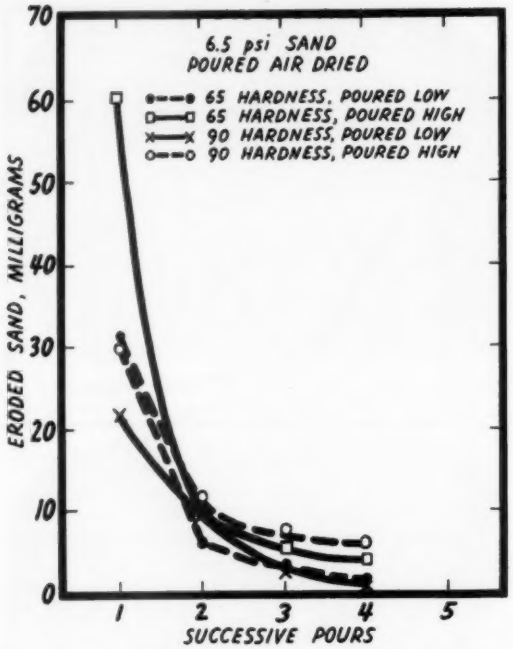

Figure 11—Amount of sand eroded with successive pours of 2.8 pounds of mercury through a ¼-inch diameter sprue.

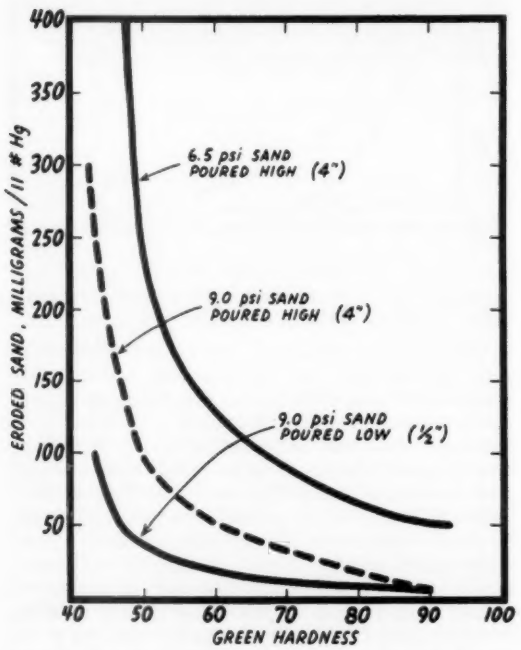

Figure 12—Summary of the data of Figures 9, 10 and 11, showing the amount of erosion resulting from pouring 11 pounds of mercury through a ¼-inch diameter sprue in relation to green hardness of the sand mass.

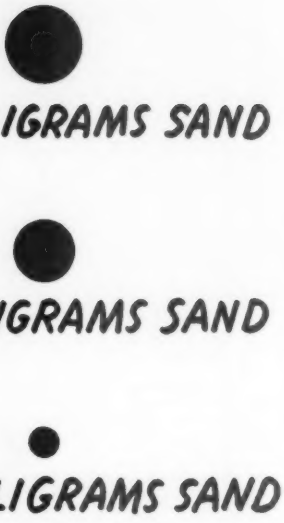

Figure 13—Circles representing the size of 10, 50 and 100 milligram cones of sand when poured on a flat surface.

The experiments were repeated using 1/8, 3/16, 3/8 and 1/2-inch diameter sprues. Erosion increased per pound of mercury with increasing diameter, but not regularly, until the sprue diameter was 1/2 inch. Erosion decreased with the 1/2-inch diameter sprue due to inability to cover the sprue walls while pouring. The 1/2-inch sprue was equivalent to pouring down a riser in production ignoring the effect of impact at the base of the riser.

It should be emphasized that the relations of Figures 9 - 12 only have relative significance. They only show the possibility for erosion of sand grains from a mold surface without thermal effects and cannot be applied literally. First, only sprues are considered in these experiments. The effect of runners and ingates is ignored. The experiments may be presenting an oversimplified picture. However, it would seem that if erosion is possible in the sprue, it is possible throughout the gating system. Perhaps a choke in the runner or in-gate would decrease erosion in the sprue, but increased erosion would result where the metal leaves the choke. This has been demonstrated in several studies of the flow of molten steel by the increased turbulence at these positions.

Figure 12 shows that practically no erosion occurs with a 9.0 psi sand rammed to 90 green hardness when poured from a low height. However, low in these experiments was ½ inch above the sprue. This height is impractical in the foundry. A low pouring height in the foundry would be closer to 4 inches. Figure 12 shows that appreciable erosion occurs at 4 inches pouring height, even at 90 green hardness, amounting to 10 milligrams of sand per 11 pounds of mercury. Ten milligrams of sand are quite visible if agglomerated in one area, as shown by the sketches

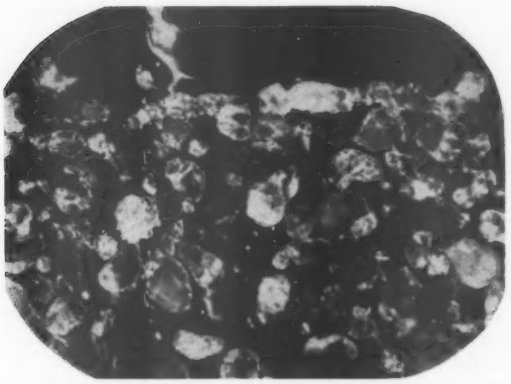

Figure 14—Production steel molding sand, 7.0 psi green strength after 10 seconds immersion in liquid steel. 25X.

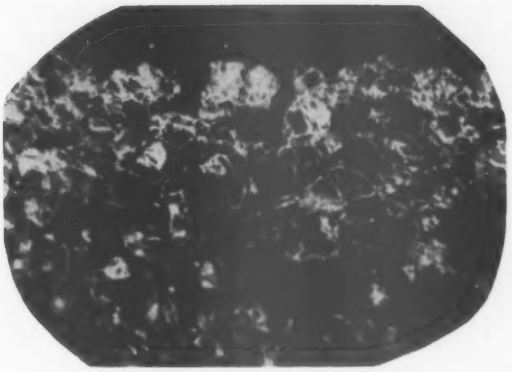

Figure 16—Same as Figure 14, but after 15 alternate immersions in liquid steel. 25X.

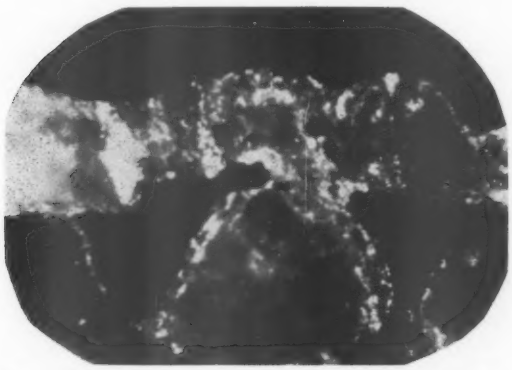

Figure 15—Same as Figure 14, but showing sintered surface at 125X.

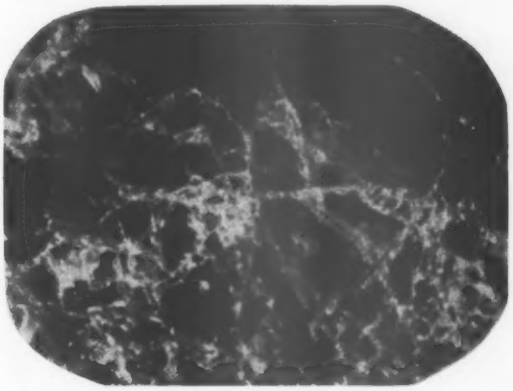

Figure 17—Same as Figure 16, but showing sintered surface at 125X.

of Figure 13. Then too, 11 pounds of mercury are equivalent to only 6.3 pounds of steel. The surface areas of the small sprues that had to be used are much smaller than production sprues. Erosion seems to be related to the surface area of the sprue, at least in these experiments. Therefore, except for glazing which will be discussed later, pure erosion in production molds could possibly be greater than shown in Figures 9 - 12.

If it is agreed that the data of Figures 9 - 12 are qualitatively correct, it is possible to summarize some of the possible factors influencing erosion:

(1) Metal flow. Pouring height in the experiments. A number of other factors will be influential in production.

(2) Sprue size. The smaller the sprue, the less area to erode, provided velocity and turbulence remain constant. Runners and in-gates are beyond the scope of this work.

(3) Bond coverage. The higher bentonite sand erodes less than the lower. A previous paper[1] showed that the amount of clay is the major factor influencing sand grain coverage by clay.

(4) Ramming is equally important to bond coverage. Figures 9 and 10 show that the higher green strength, higher bentonite sand of Figure 10 erodes more than the lower bentonite sand of Figure 9 when rammed to 60-65 green hardness. Maximum resistance to erosion of the sand itself is only attained by a combination of high bond and hard ramming. If clay content is increased with no attention paid to supplying increased ramming energy, or increased flowability, the lower rammed densities may more than cancel the advantage of increased bond coverage.

Sintering of Mold Surfaces

The sintering of sand surfaces that seems peculiar to steel probably decreases erosion to the point of no further erosion after the sintered layer becomes continuous. As has been shown previously[3] this sintered layer has excellent high temperature bond and possesses both strength and ability to deform. How-

ever, 2 to 5 seconds are required to sinter western bentonite bonded steel molding sand. At a pouring rate of 10 pounds per second, 20 to 50 pounds of steel can flow over the sand surface of a mold before it sinters. Therefore, there is a more than sufficient time interval to erode appreciable quantities of sand.

The photomicrographs of Figures 14 through 17 show sand surfaces after contact with molten steel. The surfaces are so friable until an appreciable sintered layer has formed (about 10 seconds) that it is impossible to handle them for investment. Presumably erosion can occur before this time interval. Very little difference in the sinter can be seen after about 10 seconds contact except for amount. If the sand specimen is alternately immersed in steel, simulating discontinuous metal flow over a sand surface, sintering is slower and the sand grains fragment as shown in Figure 16.

Offsetting the beneficial effect of sintering of the sand surface in contact with liquid steel is the agglomeration of the individual particles by sintering. This agglomeration is probably promoted by the presence of reoxidation products that are forming continually when liquid steel is in contact with air, or any atmosphere containing oxygen or carbon dioxide. These reoxidation products are liquid slags (manganese silicates containing varying amounts of iron oxide and alumina) and seem to promote agglomeration of eroded sand grains.

If eroded sand grains floating on the surface of the metal as individual particles are not agglomerated mechanically by eddy flow currents, or physically by sintering, they will merge with the sand surface of the mold face and be lost in the normal roughness of the cast surface. Remember, only small amounts of sand as measured in milligrams are being discussed. It is only when slight amounts of eroded sand are agglomerated at the surface, or agglomerated and trapped beneath the surface that they become visible nonmetallic defects.

The ceroxide defects are invariably mixtures of a liquid and varying amounts of angular, unfused sand grains[4]. These sand grains may have sintered enough to adhere, but they have not fused. The liquid may be furnace slag, ladle slag, or reoxidation products, but sand grains are still present. The slags, or ceroxide products, definitely pick up sand grains. Agglomeration by the liquid phase is one possible explanation for the presence of sand grains. Figures 18 and 19 show two examples. The nonmetallic defects of Figure 18 were trapped beneath the surface of a steel casting and were not in contact with the sand wall of the mold. Nevertheless, it contains at least 20 percent unfused sand grains. The nonmetallic mass of Figure 19 was picked from the center of a riser before contact with the sand wall. These two examples are typical. Koch[5] has reported on the interrelation between the ceroxide defect, eroded sand and metal flow.

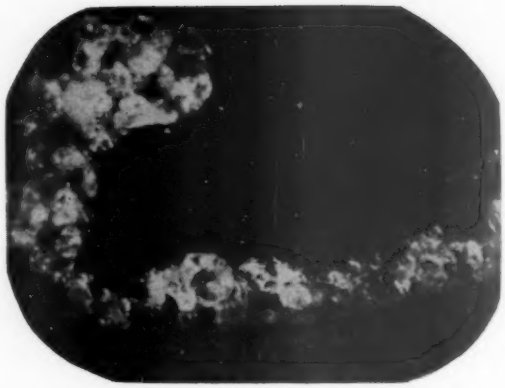

Figure 18—Nonmetallic macroinclusion composed of a liquid slag and sintered but not fused sand grains trapped below the surface of a steel casting.

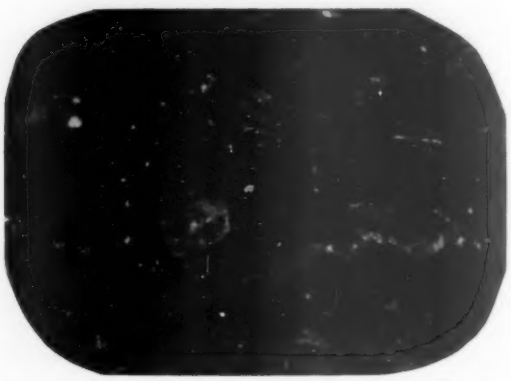

Figure 19—Nonmetallic mass picked from center of riser. SiO_2-62.3%, FeO-8.0%, MnO-18.2%, Al_2O_3-15.4%, CaO-0.0%, MgO-2.3%. Sand grains by chemical extraction 28%. Basic steel. The MgO is ladle lining. 60X.

The problem of surface and subsurface non-metallic defects with no evidence of their origin is peculiar to steel castings. It is of much less concern to the founders of the other ferrous metals. The iron foundryman is concerned with scabbing, buckling and spalling. These relatively large sand failures are of less importance in steel founding. One reason for this difference has just been discussed, sintering of the sand surface in contact with steel. The higher carbon iron alloys do not sinter, or glaze the sand surface as does steel. This sinter is a very efficient high temperature bond and should withstand any amount of expansion[3]. Drag scabs and buckles are almost unknown in the steel foundry. Cope spalls are experienced. Most occur before the sand surface is completely covered by metal. Spalls occurring in the gate system are most always due to discontinuous metal flow, covering and then uncovering the sand surface. Alternate immersion tests show slower sintering under these conditions and that spalling occurs before a continuous glaze has formed.

Superheats

The preceding paragraph may be an explanation as to why the different interest in gross scabbing, buckling and spalling; however, it does not explain the steel problem of nonmetallic macroinclusions containing sand grains without visible scabbing, buckling, or spalling. Perhaps the data of Table I furnish a clue.

Table I emphasizes the low superheat used to pour steel. If gray iron were poured at the same superheat, it would be poured under 2300 degrees F. It is almost universally agreed among iron foundrymen that defects go sky high with pouring temperatures below 2400 to 2500 degrees F. Many iron foundries pig the metal when its temperature falls below 2400 to 2500 degrees F. The problem of magnesium oxide dross in ductile iron is magnified many times when pouring temperatures fall below 2400 - 2500 degrees F, 300 - 400 degrees F superheat. Dross in ductile iron and ceroxide scum in steel are the same phenomena, reoxidation products. The chief difference, other than chemistry, is that ductile iron dross is a solid, steel ceroxide scums are liquid.

The low superheat of steel coupled with its dendritic freezing pattern tends to trap nonmetallics under the surface, even though the nonmetallics are lighter than the metal. These nonmetallics can float to the surface in the other cast ferrous metals because of the longer time the metal remains liquid after the mold is poured. If steel is poured with even the minimum superheat of the other metals, a mold entering temperature of 3030 degrees F would be required. This mold entering temperature would require tapping temperatures in excess of 3300 degrees F. The refractory problem is self evident.

There is another drawback to higher superheats for cast steel. The last column of Table I shows that the pouring temperature of steel is the only one above the "B" sintering point of bentonite-clay bonded silica sands. The "B" sintering point is the temperature when sand grains sinter to the degree that they adhere to each other and to a platinum ribbon within a time interval of 4 minutes. The point here is one of degree of time. The ceramist talks of sintering and softening points of silica-bentonite systems over 600 degrees lower than "B" sintering temperatures. The ceramist's softening points correspond roughly to the "A" sintering points. However, at the "A" sintering point, the degree of adhesion is very slight, too slight for agglomeration of individual sand grains floating on the surface of a metal as it is filling the mold cavity[6].

Agglomeration is probably also greatly affected by mold atmosphere and the presence of oxide films, or slags, either as separate phases, or due to mold atmosphere. The higher carbon gray, ductile and malleable irons are not only in contact with sands containing sea coal, but in themselves promote a reducing atmosphere. This reducing atmosphere is known to decrease glazing of the mold surface and should, therefore, decrease glazing of eroded sand grains and their agglomeration. It is possible (but not proven) that very high pouring temperatures for steel may bring eroded sand grains to the surface, but not disperse them as indivdual grains as seems possible with metals poured at lower temperatures.

The presence of visible masses of eroded sand grains is possible with the lower melting metals because of eddy currents while the mold cavity is filling without agglomeration due to sintering. Visible masses of eroded sand are also possible if there is a great amount of erosion. The important point is that perhaps much smaller amounts of eroded sand become visible because of the higher pouring temperature and lower superheat of cast steel.

If the nonmetallics cannot be dispersed, it seems necessary to eliminate them at the source. A highly bonded sand, high rammed density, proper gate systems, with careful pouring will minimize, but perhaps not eliminate sand erosion as one possible cause of nonmetallics. It may be that a different approach is needed for further improvement. One possible approach is an intensive study of rammed sand surfaces.

TABLE I—A Comparison of Pouring Temperatures and Superheats of Various Metals

Metal	Liquidus Temperature Degrees F	Mold Entering (Pouring) Temperature Degrees F	Superheat Degrees F	Relation of Pouring Temperature to "B" Sintering Point of Molding Sand, 2850°F (3) (6)
Steel, 0.25%C	2780	2760 - 3000	0 - 220	–70 to –150
Malleable Iron	2350	2600 - 2750	250 - 400	–100 to –250
Gray Iron	2150	2400 - 2700	250 - 550	–150 to –450
Ductile Iron	2100	2400 - 2700	300 - 600	–150 to –450

TABLE II—The Density of Sand Surface as Determined by Two Different Methods

	25% Silica Flour	Unbonded Sand	Molding Sand	Molding Sand	Molding Sand	Shell Sand
Density by Grid Method, % Solid	67	61	51	56	55	60
Density by Weight, % Solid	62	63	55	54	55	63

REFERENCES

1. Caine, J. B., King, E. H., Schumacher, J. S., "A Microscopic Study of the Bonding of Steel Foundry Sands by Clays," *Journal of Steel Castings Research,* No. 16, January 1960.
2. Caine, J. B., "A Study of 'Burnt On' or Adhering Sand," *Trans. AFS,* Vol. 51, (1944) p. 647.
3. Caine, J. B., "A Study of the Behavior of Molding Sand When in Contact with Liquid Steel," *Foundry,* Vol. 75, No. 17 (1947) p. 72.
4. Vingas, G. J., and Caine, J. B., "Causes and Mechanics of the Scum Defect," *Foundry,* June 1959, p. 94.
5. Koch, N. F., "A Study of the Ceroxide Cope Defect and Eroded Sand," *Steel Foundry Facts,* No. 168, July 1956.
6. Report of the Subcommittee on Sintering Test, Foundry Sand Research Committee, 1941 - 1942, *Trans. AFS,* Vol. 50 (1943) p. 785.

APPENDIX

The sand surfaces shown have been prepared by saturating the sample with a thermosetting plastic, hardening the plastic by heating at 150 - 200 degrees F for about 24 hours, and polishing like a metal sample. Oblique, or a combination of oblique and vertical illumination was used.

Figure 20—Sand specimen with superimposed grid to determine density. 25X.

The density of any area of the prepared sand surface can be determined fairly accurately by superimposing a grid as in Figure 20. The percent solid is estimated in a number of squares (at least 20, preferably 50) and averaged. The squares show anything from zero to 100 percent solids. If enough squares are averaged, a relatively accurate estimate can be made of any area of the photomicrographs. Table II shows a number of estimates of density determined by averaging 50 squares randomly selected from photomicrographs compared with the density determined by weight and volume of the gross sample.

SFSA RESEARCH REPORT No. 45
PACKING OF STEEL FOUNDRY SANDS

Very little systematic work has been done on the packing of aggregates as related to steel foundry molding sands. The Technical Research Committee of SFSA recognized the need for research on this subject and initiated studies to investigate certain aspects of the mechanical behavior of steel foundry molding sands. Experimental studies were carried on in the Foundry Division at Massachusetts Institute of Technology under the direction of Professor H. F. Taylor. The report containing these results was reviewed by the Technical Research Committee and submitted to Dr. W. G. Lawrence of Alfred University to review, revise and edit as a research report for the SFSA member companies.

In addition to experimental data on the packing of sand-water mixtures, sand-bentonite-water mixtures, grain size distribution, and hot deformation, the report also contains a comprehensive review of the literature on the basic concepts of particle packing.

Screened and blended sand to exact proportions to produce varying packing characteristics showed ex-

perimentally the effect of grain distribution on density and other mechanical phenomena as follows:

Green Properties	Increased by:
Bulk Density	Wide size distribution Small grain size
Flowability	Low clay contents
Hardness	Ramming Small grain size Wide grain size distribution
Compressive Strength	Wide grain size distribution Ramming High clay content Low water content
Deformation	Wide grain size distribution Coarse grain size High clay content High water content

Hot Properties	Increased by:
Expansion:	
Maximum expansion	Small grain size
Time to maximum expansion	Small grain size
Time of contraction	Increasing clay content Decreasing temperature
Final expansion	Increasing temperature
Time to final expansion	Decreasing temperature
Hot compressive strength	Increasing clay content Decrease grain size Increase density Temperature (max. 1650 degrees F)
Hot deformation	Decrease density Increase clay content Temperature (max. 2000 degrees F)

MAGNETIC PROPERTIES OF CAST CARBON STEELS—PART II

by

W. J. Jackson, M. Sc., A.R.I.C., A. I. M.

Part I of this report appeared in the preceding issue of the Journal of Steel Castings Research.

Part II—The Development of Optimum Magnetic Properties for a Minimum Heat Treating Time.

For any given carbon content, the measure of improvement in magnetic permeability resulting from annealing, as compared with normalizing, has been demonstrated. If, however, advantage is to be taken of the superior magnetic properties of fully annealed material, and heat treating times are to be kept to a minimum, it is important to know the temperature at which a furnace charge can be withdrawn and air cooled, without impairment of magnetic properties.

With this end in view, a further series of tests were carried out to determine the effect of furnace withdrawal temperature on magnetic permeability. In addition, one test was made to determine the effect of slow cooling through the austenite transformation temperature range.

Provision of Test Material

The steel used in this investigation was made by the Tropenas Converter process. Six plain cylindrical test blocks (4½-inch diameter, 8 inches high) were cast. The analysis of the blocks is given in Table VII.

Three "slices," approximately 1 inch thick, were cut from the bottom portion of three of the castings. Seven of these slices were subsequently used in this investigation. It was found necessary to carry out the heat treatment in three separate batches, on account of the internal dimensions of the furnace used. Furnace conditions were therefore controlled to be as near as possible the same during the treatment of each batch.

TABLE VII—Chemical Analysis of Carbon Steel Used in Part II

Composition, percent				
C	Si	Mn	S	P
0.17	0.26	0.38	0.021	0.042

In each case the slices were charged into a cold furnace, which took approximately 4 hours to reach a temperature of 1740 degrees F and were held at this temperature for 4 hours. The slices were then singly withdrawn from the furnace as it cooled, at the temperatures shown in Table VIII, and allowed to cool in air. The total time that each slice remained in the furnace was therefore, 8 hours plus the furnace time given in Table VIII.

The heat treatments carried out on batches 1 and 2 were such as to give various withdrawal temperatures from the furnace immediately between normalizing and annealing. The treatment of batch 3 gave a normal furnace cool from 1740 degrees F to 1380 degrees F, a retarded cooling from 1380 degrees F to 1200 degrees F lasting 5 hours, whereupon the slice was withdrawn and air cooled. One magnetic test ring was then machined from each slice. The mean hardness of each ring, given in Table VIII, was determined after completion of the magnetic testing.

TABLE VIII—Details of Various Experimental Heat Treatments, and Resulting Hardnesses Obtained

Heat Treatment Batch	Time in furnace after soaking period - hrs.	Temp. of withdrawal, °F	Mean Vickers Diamond Hardness of ring (load 30Kg)
1	0	1740 (norm.)	135
	2-1/3	1290	135
	3-1/2	1110	130
2	5-1/2	930	127
	7-1/2	750	127
	9-2/3	570 (ann.)	126
3	7*	1200	124

* 5 hours to cool through 1380-1200 degrees F

TABLE IX—Effect of Furnace Withdrawal Temperature and Slow Cooling Through the Critical Temperatures of a 0.17% Cast Carbon Steel

Flux Density B (Gauss)	Slow Cool 1380°F - 1200°F & Withdrawn		Withdrawn at 570°F (Annealed)		Withdrawn at 750°F		Withdrawn at 930°F		Withdrawn at 1110°F		Withdrawn at 1290°F		Withdrawn at 1740°F (Normalized)	
	H(Oer.)	μ Max.	H(Oer.)	μ Max.	H(Oer.)	μ Max.	H(Oer.)	μ Max.	H(Oer.)	μ Max.	H(Oer.)	μ Max.	H(Oer.)	μ Max.
5,000	2.35		2.50		2.65		2.65		2.70		3.05		3.70	
10,000	5.75	2100 at	6.25	2090 at	6.70	1900 at	6.70	1900 at	7.05	1895 at	7.70	1895 at	9.95	1395 at
14,000	16.5	6000 Gauss	19.0	5750 Gauss	22.0	5600 Gauss	22.0	5600 Gauss	26.0	5400 Gauss	22.0	5700 Gauss	36.0	6000 Gauss
15,000	25.0		29.0		35.0		35.0		41.0		31.0		62.0	
16,000	42.5		47.0		58.0		58.0		72.0		48.0		102.0	
17,000	70.0		78.0		97.0		103.0		135.0		81.0		....	
18,000	120.0		133.0		170.0		....		....		....		....	

Test Results

Magnetization curves for each material were determined, the first part of each of these curves (up to 8 oersteds) being shown in Figure 6. It will be seen that the material slowly cooled through the tempearture range 1380 - 1200 degrees F gave superior magnetic properties at all field strengths tested. The remaining material exhibited decreasing permeability as the withdrawal temperature increased from annealing (570 degrees F) to normalizing (1740 degrees F), with the exception of the material withdrawn at 1290 degrees F. The latter showed superior permeability to the annealed material at field strengths above 100 oersteds, falling off below this value until at field strengths lower than 40 oersteds, permeability was only slightly superior to that of the normalized material. Results from the magnetization curves are given in Table IX, from which it may be seen that maximum permeability is progressively lowered as withdrawal temperature increases.

Discussion

The results indicate that superior magnetic properties, at shorter heat treatment times than required for full annealing, were obtained at high field strengths in the material withdrawn at 1290 degrees F, and at all field strengths in the material slowly cooled through 1380 - 1200 degrees F. In the case of the latter, the slow cooling time of 5 hours could possibly be reduced by isothermally annealing at a temperature very slightly lower than the A_1 temperature. This however, would involve prior determination of the isothermal transformation curve of the particular steel being treated, so that sufficient time

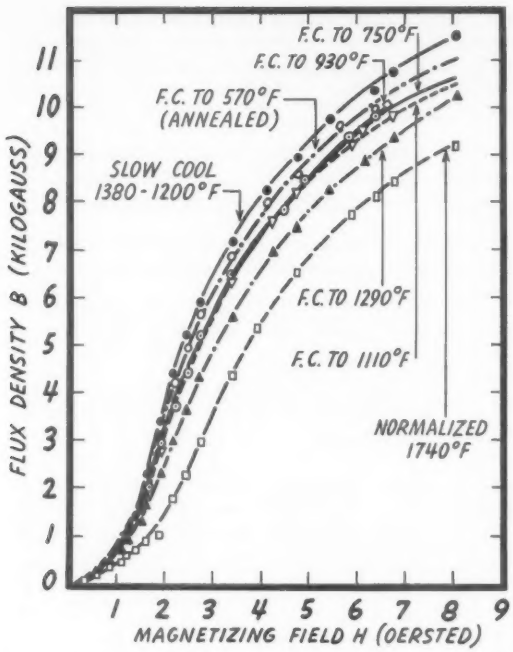

Figure 6—Magnetization curves showing relative positions of curves at field strengths lower than 8 oersteds.

may be given at temperature to allow the transformation to go to completion.

An advantage of isothermal annealing, over full annealing, lies in the fact that the furnace temperature need not be lowered below 900 - 1100 degrees F, and that the next furnace charge more rapidly attains annealing (austenitic) temperature.

The reason for the improved magnetic properties (at higher magnetizing fields) of the material withdrawn at 1290 degrees F is not at all clear, although it is not uncommon for magnetization curves to cross at the higher field strengths. The average hardness of this material was the same as that of the normalized material, although their microstructures differed considerably, as shown in Figure 7.

It appears from the microstructure that upon withdrawal at 1290 degrees F, the austenite transformation had not gone to completion. The permeability of this material would therefore be expected to be slightly inferior to that of the material withdrawn at 1110 degrees F, which, in fact, it is at lower magnetizing fields.

In the case of the material withdrawn from the furnace at each of the temperatures 1110, 930, 750 and 570 degrees F, there was a slight indication of an increasing ferrite grain size, and a tendency for pearlite to be coarser as the temperature of with-

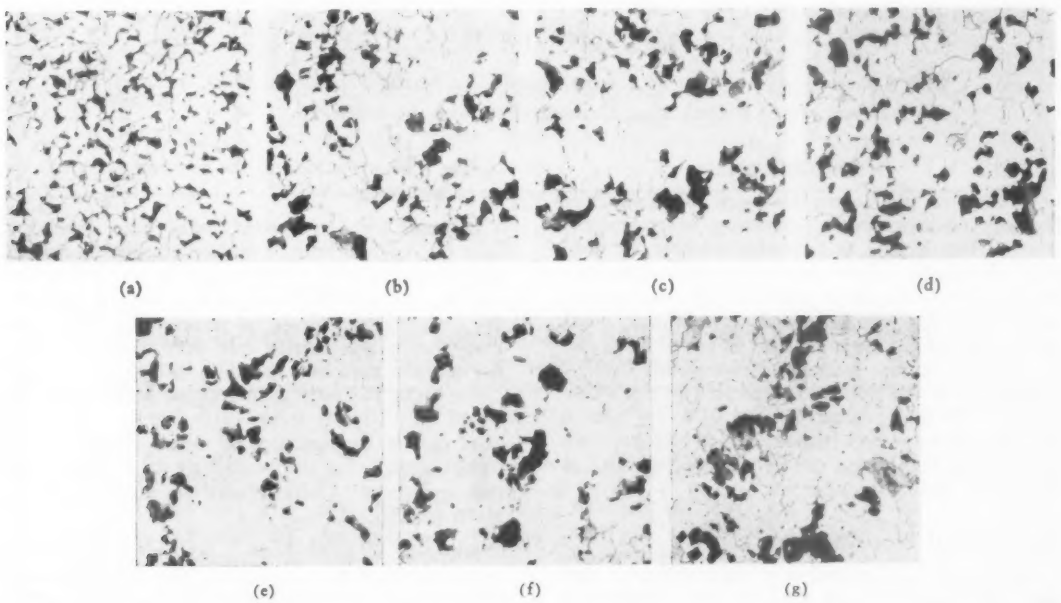

Figure 7—Microstructure of a 0.17 percent carbon steel, subjected to the various heat treatments used in Part II. (Etched in 2 percent nital, 120X)

(a) Normalized 1740 degrees F, AC
(b) F.C. 1290 degrees F, AC
(c) F.C. 1110 degrees F, AC
(d) F.C. 930 degrees F, AC
(e) F.C. 750 degrees F, AC
(f) F.C. 570 degrees F, Annealed
(g) Slow Cool 1380 - 1200 degrees F, AC

drawal decreased. This microstructural observation is in accordance with the determined magnetic properties. However, the material slowly cooled through 1380 - 1200 degrees F exhibited a slightly smaller grain size, and a slightly greater carbide dispersion than the fully annealed (withdrawn at 570 degrees F) material. It therefore appears that the magnetic properties of a low carbon steel are not entirely dependent on the microstructure as revealed by etching.

Conclusions to the Report

For the cast carbon steels, under the experimental conditions described, it has been shown that:

1. Magnetic permeability is decreased by increasing the carbon content from 0.10 percent to 0.34 percent, irrespective of heat treatment.

2. Annealing develops higher maximum permeability than normalizing. The maximum permeabilities of the 0.10, 0.14 and 0.19 percent carbon as-cast steels were intermediate between the annealed and normalized, while the maximum permeabilities of the 0.24 and 0.34 percent carbon as-cast steels were the lowest of all steels tested.

3. In the range of flux density at which electrical equipment normally operates, the magnetic properties of annealed material are superior to those of normalized material, which in turn are superior to those of as-cast material.

4. A relationship between tensile strength and magnetic properties of steels in the annealed and normalized conditions has been demonstrated.

5. Optimum magnetic properties for a minimum heat treatment time were obtained by:

a) slowly cooling through the temperature range 1380 - 1200 degrees F and then air cooling, and

b) at higher magnetizing fields, only by furnace cooling to 1290 degrees F, then air cooling.

The former treatment, as well as giving higher permeabilities at all field strengths than fully annealed material, offers the possibility of economy in furnace time and heat.

THE EFFECTS OF RESIDUAL ELEMENTS ON THE MAGNETIC PROPERTIES OF CARBON STEEL CASTINGS

by

W. J. Jackson* and E. J. Ridal**

This report is a summary of a paper published in the February, 1960, issue of the Journal of the British Steel Castings Research Association.

INTRODUCTION

In view of the known tendency for residual or impurity elements to be increasing in commercial scrap, it was decided to determine whether the presence of certain residual elements was particularly harmful to the magnetic properties of high permeability steel castings. The work was planned, therefore, to determine the individual effects of a number of elements, in the amounts indicated in Table I. In addition, it was decided to include two steels containing 0.55 - 0.65 percent Mn and 0.90 - 1.0 percent Mn, because some steel founders would prefer to work to a higher manganese content than is allowed in B.S. 1617, namely 0.50 percent.

Experimental Procedure

The charge was melted in a high frequency furnace and brought to the required steel composition by adding carbon as white iron, and manganese and silicon as ferro alloys. The "residual" elements were added as the pure metals (i.e., Sn, Ni, Pb, Cu) or as ferro alloys (i.e., Cr, Mo, Ti, V). Lead in the form of fine shot was added to the pouring stream as the mold was being filled.

In some cases, 70-pound heats were made and split into two portions, a further addition of residual element being made to the second portion, (i.e., 13A and B, 15A and B, 16A and B, and 17A and B). For the remainder, single 30-pound heats were made. Deoxidation was carried out with aluminum wire, the quantity used corresponding to 2 lb/ton of steel. Throughout the series, the pouring temperature deviated only slightly from 2910 degrees. The steels were cast in dry sand molds into a cylindrical test block suitable for the machining of magnetic test ring specimens. Chemical analyses of the steels are given in Table II.

Slices cut from the bottom portion of each of the test blocks were heat treated together using the treatment previously found to give optimum permeability (see the preceding article, "Magnetic Properties of Cast Carbon Steels—Part II). That is, the furnace charge was heated to 1740 degrees F and held at temperature for 4 hours, whereupon the power was switched off and the charge cooled in the furnace to 1380 degrees F. Cooling from this temperature

* Head and ** Senior Technical Assistant, respectively, Metallurgy Section, British Steel Castings Research Association.

TABLE I—Residual elements investigated individually.

	Element, %							
	Ni	Cr	Mo	Cu	Sn	Pb	Ti	V
Low Range	.12–.18	.12–.18	.035–.045	.12–.18	.015–.020	.010–.015	.010–.015	.010–.015
High Range	.32–.38	.32–.38	.060–.080	.32–.38	.030–.040	.....	.040–.050	.050–.060

TABLE II—Results of analyses of test block castings.

Heat No.	Added Element	Composition, %												
		C	Si	Mn	S	P	Ni	Cr	Mo	Cu	Sn	Pb	Ti	V
12A	Blank	.12	.20	.39	.015	.017	.005	.01	.020	.10	.006	...	...	...
13A	Tin	.13	.27	.38	.015	.019	.008	Trace	.011	.10	.019	...	...	...
13B	Tin	.13	.22	.34	...	...	...	...	...	...	.039	...	...	...
15A	Manganese	.14	.28	.65	.011	.013	.014	Trace	Trace	.10	.006	...	...	...
15B	Manganese	.14	.21	.93	.010	.014	...	...	...	...	...	...	...	...
16A	Nickel	.12	.25	.39	.014	.017	.14	Trace	.021	.08	.006	...	...	...
16B	Nickel	.12	.16	.33	.014	.017	.38	...	...	.07	...	...	...	...
17A	Chromium	.13	.21	.34	.014	.017	.012	.11	.023	.10	.006	...	...	...
17B	Chromium	.13	.19	.40	.014	.018	...	.31	..,	.10	...	...	...	...
19	Lead	.12	.23	.28	.016	.018	.013	.01	.023	.10	.006	.016*	...	...
21	Molybdenum	.12	.31	.38	.014	.016	.013	Trace	.045	.08	.006	...	...	...
22	Molybdenum	.12	.33	.32	.015	.018	.012	Trace	.075	.10	.008	...	...	...
33	Copper	.12	.42	.39	.011	.019	.020	Trace	Trace	.34	.010	...	...	...
103	Blank	.14	.36	.37	.007	.020	.017	.05	Trace	.01	...	...	Trace	.026
106	Titanium	.13	.31	.33	.008	.020	...	...	...	...	...	...	.015	...
107	Titanium	.14	.32	.35	.007	.020	...	...	...	...	...	...	.045	...
108	Vanadium	.13	.33	.38	.006	.022	...	...	...	...	...	...	Trace	.059

* Spectrographic

TABLE III—Data from magnetization and hysteresis curves for material heat treated by holding 4 hours at 1740 degrees F, slowly cooling through 1380 - 1200 degrees F, and air cooling from 1200 degrees F.

Flux Density B (gauss)	Magnetizing Field, H (oersted)																
	12A Blank	13A .019% Sn	13B .039% Sn	15A .65% Mn	15B .93% Mn	16A .14% Ni	16B .38% Ni	17A .11% Cr	17B .31% Cr	19 .016% Pb	21 .045% Mo	22 .075% Mo	33 .34% Cu	103 Blank	106 .015% Ti	107 .045% Ti	108 .059% V
5,000	2.1'	2.1	2.3	2.2	2.5	2.0	2.1	2.1	2.1	2.1	2.1	2.1	2.2	2.1	2.2	2.2	2.2
10,000	4.4	4.8	5.1	5.6	6.2	4.6	4.7	4.8	5.1	4.9	5.1	5.1	5.0	4.9	4.9	5.1	5.4
14,000	14.0	16.0	17.0	18.0	19.0	17.5	16.0	18.4	16.0	17.0	15.5	15.5	13.3	16.0	16.3	18.5	18.2
15,000	22.2	27.0	25.0	29.8	31.0	26.8	24.0	31.5	26.2	28.5	24.8	24.8	22.0	27.0	28.0	31.0	31.0
16,000	41.0	47.5	45.0	49.0	55.0	48.0	44.0	58.0	50.2	52.0	44.0	44.0	37.0	50.0	50.0	51.0	56.5
17,000	75.0	91.0	91.0	90.0	98.0	91.5	84.0	...	91.0	97.0	85.5	85.5	72.0	93.0	101.0	82.5	...
μ max.	2620	2580	2400	2340	2050	2720	2720	2620	2520	2580	2550	2550	2410	2580	2500	2490	2480
B_r (gauss)	9900	...	...	9900	10850	...	...	...	...	...	...	...	...	...	...	...	...
H_c (oe)	1.7	...	...	1.8	2.3	...	...	...	...	...	...	...	...	...	...	...	...

to 1200 degrees F was then retarded so that the cooling rate was approximately 35 degrees F per hour. At 1200 degrees F, the slices were withdrawn from the furnace and air cooled.

Ring test specimens were machined from the slices. Using the method of reversals, magnetization curves were drawn for each steel. Full hysteresis curves were drawn for the blank (12A) and for the two steels of high manganese content (15A and B). Data from all the curves are grouped for comparison in Table III.

Effect of Individual Elements

NICKEL—The B-H curves for heats 12A, 16A and 16B indicated that the addition of nickel lowers magnetic properties, and that a low content of nickel (0.14 percent) is more deleterious than a high content (0.38 percent) at field strengths above 10 oersteds. A second series of steels was made with similar nickel contents. The B-H curves indicated that the addition of nickel raises magnetic properties, which is contrary to the effect noted in the first series.

In each series, the microstructures of the nickel-containing steels were similar to that of the blank, and the average hardness of the ring test specimens was reasonably constant. It was thought, therefore, that some variable was being introduced during melting, and that this factor was having a greater influence on magnetic properties than the small amounts of nickel that had been added. Vacuum fusion gas analyses were carried out on these six steels. The gas contents were rather variable, and it could not be shown that the gas content directly affected magnetic properties.

CHROMIUM—The effect of chromium appeared to be similar to nickel in the first series of steels, i.e., chromium lowered magnetic properties. A similar anomalous result was also observed, in that the lower chromium content (0.11 percent) appeared to be more deleterious than a higher chromium content (0.31 percent), except only at field strengths between 2 and 9 oersteds. While the hardness of the two steels was the same, it was noted that the pearlite was slightly coarser in the steel of higher chromium content.

MOLYBDENUM—The addition of molybdenum had the effect of slightly lowering magnetic properties. Increasing the molybdenum content from 0.045 to 0.057 percent did not have any significant effect on the B-H curve. The addition of molybdenum did not alter the microstructure, but increased the hardness slightly.

COPPER—Copper was only added in the "high" range, as the iron charge used in the first series of steels already contained 0.10 percent. Increasing the copper content to 0.34 percent had virtually no effect on magnetic properties. The microstructure appeared to contain less carbon than would be expected from the analysis, although the hardness was slightly increased.

TIN—The effect of tin was similar to that of molybdenum. Additions of 0.019 and 0.039 percent lowered magnetic properties by approximately equal amounts. The higher tin content, however, lowered the maximum permeability more than any other individual addition.

LEAD—The effect on the B-H curve of adding 0.016 percent lead was surprisingly large in view of the fact that it is insoluble in steel. Lead could not be detected in metallographic specimens and had no effect on microstructure or hardness.

TITANIUM—The addition of titanium had very little effect on magnetic properties. In fact, at about 50 oersteds, the curve for the steel containing 0.045 percent Ti crossed the other curves, and became slightly superior to both the blank and the steel containing 0.015 percent Ti. The grain size of the titanium containing steels was slightly smaller than that of the blank. The average hardness was not significantly affected by the titanium additions.

VANADIUM—Vanadium was added only in the "high" range, as the iron charge used in the second series of steels already contained 0.026 percent vanadium. The effect of this addition was to slightly lower the magnetic properties. The microstructure was unaltered, although the average hardness appeared to be lowered.

MANGANESE—The addition of manganese up to 0.93 percent had the effect of lowering the B-H curve. The results indicate that manganese up to 0.6 percent does not have a serious effect on coercivity, but maximum permeability and H value at 17,000 B (i.e., typical working range of electrical equipment, where high flux densities are required) are impaired. The limit of 0.5 percent Mn given in B.S. 1617 would appear to be justified.

Effect of Combined Elements

NICKEL, CHROMIUM AND MOLYBDENUM—Since in practice residual amounts of several elements are likely to be found in commercial scrap, it was decided to add nickel, chromium and molybdenum together. Two 0.13 carbon heats were made with analyses of .22 percent Ni, .23 percent Cr, .035 percent Mo and .24 percent Ni, .24 percent Cr, 0.23 percent Mo for comparison with a blank heat containing only traces of nickel, chromium and molybdenum.

The unexpected result was that the combined addition improved magnetic properties slightly. It can only be concluded that the combined presence of these three elements is beneficial. It should be pointed out, however, that the maximum permeability was lowered very slightly in both heats.

ALUMINUM DEOXIDATION—Since most steel castings are deoxidized with aluminum, it was thought that the effect of this element on magnetic properties should be examined. Consequently, a heat was made using 4 lb/ton CaSiMn for deoxidation, instead of 2 lb/ton aluminum. Unfortunately, this steel was slightly higher in carbon than others in the series. (This heat was repeated, and the carbon content was again slightly high.) The B-H curve of this heat was consequently lower than that of the blank heat, but only to the extent which may be expected from the higher carbon content. It may be indirectly concluded, therefore, that deoxidation with 2 lb/ton aluminum has no harmful effect on magnetic properties.

Effect of Microstructure

All the steels used in this investigation were assessed for the parameters described below in an attempt to ascertain whether a statistical correlation could be determined between each parameter and a magnetic property of the steels.

INCLUSION CONTENT—The polished micro-sections were projected, at a magnification of 850X, on to a grid of millimeter squares. The number of grid intersections covering each inclusion in the field selected was counted and assessed as a percentage of the total area of the grid. Sixty counts were made on each steel, and the average taken.

FERRITE GRAIN SIZE—This was assessed by comparing the ferrite grains with a transparent A.S.T.M. grid.

PEARLITE LAMELLAR SPACING—This was determined by projecting on to a millimeter scale at a magnification of 4550X. The average spacing for each pearlite patch was measured.

PEARLITE PATCH SIZE—This was determined by projecting on to a grid of millimeter squares, at a magnification of 250X, and counting the number of intersections covered by a patch of pearlite. Ten patches were counted in each specimen and the average taken.

FERRITE-PEARLITE RATIO—This was determined by projecting on to a grid of millimeter squares at a magnification of 850X. It was found that sufficient accuracy was obtained by counting the intersections of the 10 mm squares. Sixty counts were made on each specimen to assess the average percentage area of the pearlite, and the percentage area of ferrite obtained by difference. The ratio of the area of ferrite to the area of pearlite was then calculated.

In each case, there was no correlation between any of these parameters and magnetic properties. The relationship with the highest sensible correlation was ferrite-pearlite ratio versus H value at 15,000 B, but even this was of a low order.

Conclusions

Under the experimental conditions reported, the following effects were noted on high permeability cast steel:

(a) The addition of individual residual alloying elements slightly impaired magnetic properties.

(b) The combined addition of nickel, chromium and molybdenum slightly improved magnetic properties, except at low field strengths.

(c) Increasing manganese to 0.93 percent had only a small effect on remanence and coercivity, but lowered maximum permeability and flux density at the higher magnetizing fields.

(d) Deoxidation with 2 lb/ton aluminum did not affect magnetic properties.

It is generally concluded that cast steels of low residual alloy content have their magnetic properties slightly impaired by increasing the metallic impurity, although the investigation has shown that there were some anomalies, the causes of which were not determined.

Nevertheless, in steels where the magnetic properties were lowered, the order of impairment was small when compared to differences that can be produced by heat treatment. It is considered, therefore, that residual alloying elements, when present in the ranges investigated, need cause no great concern in the manufacture of high permeability castings.

ABSTRACTS OF FUNDAMENTAL PAPERS ON STEEL CASTING RESEARCH

Based on a review of the current literature on technical research subjects. (Copies of these articles available from original publishers only.)

Gases

Heide, O., "Porosity in Steel Castings," 26th International Foundry Congress, Madrid, 1959, Paper 13. A technique is described of sampling liquid steel at the end of its course through the mold, developed especially for these tests. In bentonite sand molds no inter-dependence between the hydrogen absorption of the steel and the moisture content of the sand was found. The pouring temperature was, however, found to affect the hydrogen absorption of the steel, the higher pouring temperature causing a greater degree of hydrogen absorption. The porosity of steel was found to be dependent on the final hydrogen content and on the silicon or silicon and aluminum content.

Intergranular Fracture

Woodfine, B. C., and Quarrell, A. G., "Effect of Al and N on the Occurrence of Intergranular Fracture in Steel Castings," Journal of the Iron and Steel Institute, August 1960. An investigation has been made into the occurrence of intergranular fracture of low alloy steel castings of varying aluminum and nitrogen contents, and it has been confirmed that this type of fracture is associated with the precipitation of segregation of aluminum nitride at the austenite grain boundaries on slow cooling below about 2100 degrees F. An explanation is offered for the absence of intergranular fracture from steels containing very large amounts of aluminum nitride, and it is shown that intergranular fracture can be avoided by deoxidizing with titanium, zirconium, or titanium in combination with aluminum.

Solidification

Malek, M., "Effect of the Pouring Temperature on the Formation of Shrinkage Cavities at Junctions of Thin-Walled Steel Castings," SLEVARENSTVI, December 1959. A description of tests carried out to determine the influence of the pouring temperature on the formation of shrinkage cavities at T-junctions of flanged medium carbon steel castings having a wall thickness of 12, 16 and 20 mm. It was found that the zone of shrinkage cavities and the size of the cavities is largely dependent on the pouring temperature and that the area of inhomogeneity at the juncture decreases with increasing pouring temperatures. The most advantageous pouring temperature was found to lie between 2840 and 2860 degrees F.

Testing

Zandman, F., "Stress Analysis with a Photoelastic Coating," METAL PROGRESS, November 1960. Direct observation of the stress distribution of an actual part under load is possible with this coating technique. The direction and magnitude of principal stresses can be easily determined and test results can be recorded by color photography.

Testing

"X-Ray Diffraction Measures Stress Even in Hard Steel," SAE JOURNAL, January 1961. X-ray measurement of residual stress in hard steels by the two-exposure method and use of diffractometers has an absolute accuracy of 5000 - 10,000 psi. It measures relative stress levels with a precision of 4000 - 5000 psi. Stress measurement by X-ray diffraction is based on measuring strain—and then converting it to stress by equations developed in the classical theory of elasticity. This method will detect elastic strains only, since it is fundamentally a measure of interatomic spacings which are altered by elastic stresses.

Properties and Testing

Johnson, H. H., and Stout, R. D., "Comparison and Analysis of Notch-Toughness Tests for Welded Steel," WELDING RESEARCH SUPPLEMENT, November 1960. This article is a survey of the literature on the notch toughness of welded steel. It attempts to clarify the degree of correlation among the various tests that have been devised. The most important conclusion obtained from this study is that there is no single notch-toughness test which can predict the transition temperature of a specific structure, for that temperature depends at least partially upon factors which notch-toughness tests are inherently unable to evaluate, such as structure design and fabrication procedures.

Gases

Neu, M. G., "Hydrogen in Steel," FOSECO, NO. 6, April 1960, published by Foundry Services International, Ltd. A simple method of inert gas flushing of steel melts in the ladle has been investigated with the object of reducing the hydrogen content of the metal. The method is based on the evolution of a mixture of carbon monoxide and dioxide from Logas 11 blocks held submerged in the liquid steel. A number of techniques for applying the blocks have been satisfactorily developed and melts varying in weight from 350 pounds to 120 tons have been treated.

Gases

Troiano, A. R., "Embrittlement by Hydrogen and Other Interstitials," METAL PROGRESS, February 1960. Hydrogen embrittlement is sensitive to strain rate and temperature. The kinetics of delayed failure involve an incubation period for initiation, followed by discontinuous crack propagation to catastrophic failure. Delayed failure and slow strain rate embrittlement have been observed in metals other than steels and can be brought about by interstitials other than hydrogen. Slow strain rate embrittlement, strain-aging embrittlement, and brittle delayed failure are all manifestations of the same basic phenomenon.

Metal-Mold Reactions
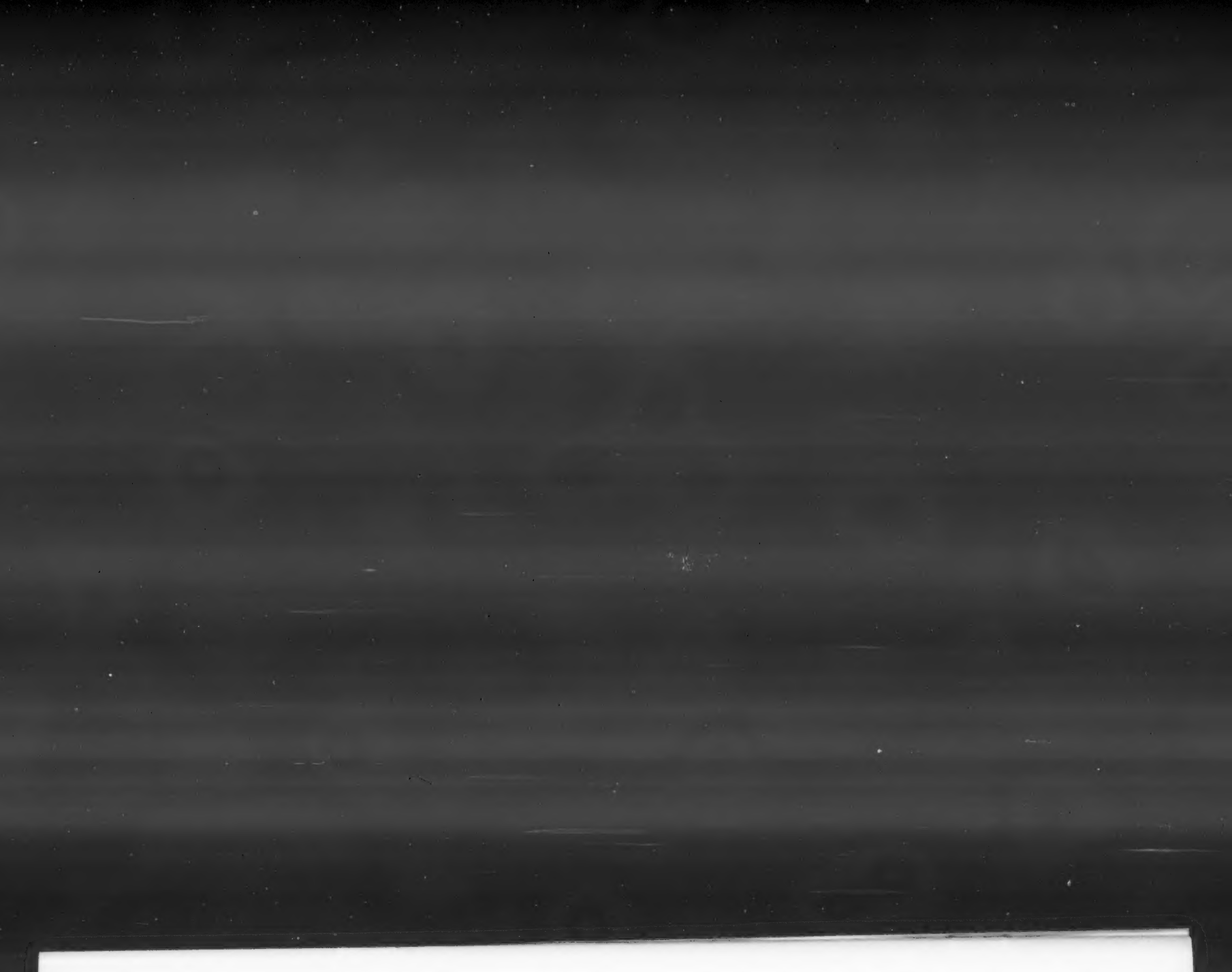
Colligan, G. A., Van Vlack, L. H., and Flinn, R. A., "Factors Affecting Metal-Mold Reactions," MODERN CASTINGS, January 1961. In order to correlate the equilibrium data with actual practice, the effect of manganese additions and atmosphere on interface reaction was qualitatively evaluated. The effect of an oxidizing mold atmosphere was demonstrated in the green sand castings by extensive reaction at the interface. Manganese additions caused extensive silicate melt formation. The reaction became more pronounced with increasing manganese content in green sand molds.